



Crystal Structure Refinement of Galvinoxyl Radical, $C_{29}H_{41}O_2$, Based on Synchrotron X-ray Powder Diffraction and Rietveld Method

Hwo-Shuenn Sheu^{a,b} (許火順), Chih-Hao Lee^a (李志浩),
Yu Wang^{*a,b} (王瑜) and Long Y. Chiang^c (江隆永)

^aSynchrotron Radiation Research Center, Hsinchu Science-Based Industrial Park,
Hsinchu, Taiwan 30077, R.O.C.

^bDepartment of Chemistry, National Taiwan University, Taipei, Taiwan 10764, R.O.C.

^cCenter for Condensed Matter Science, National Taiwan University, Taipei, Taiwan 10764, R.O.C.

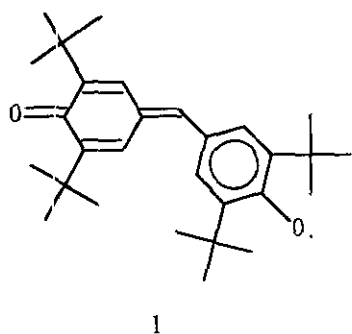
High-resolution X-ray powder diffraction with synchrotron radiation coupled with Rietveld analysis has been used recently as one of the best way to obtain structural information from a powder specimen. Molecular and crystal structures of the galvinoxyl radical ($C_{29}H_{41}O_2$) were studied by means of powder diffraction using NSLS (National Synchrotron Light Source) with $\lambda = 1.5855 \text{ \AA}$ and a rotating anode with Cu K α radiation. The space group of the crystal is C 2/c with refined lattice parameters $a = 23.786(1)$, $b = 10.8611(4)$, $c = 10.6766(4) \text{ \AA}$, $\beta = 106.634(3)^\circ$, $Z = 4$. The peak shape was fitted with a pseudo-Voigt profile function. The preferred orientation is along the $\langle 011 \rangle$ direction of the needle-like crystals. Final refinements were converged to give agreement indices $R_p 0.08$ and 0.17 respectively for synchrotron radiation and rotating anode data. The fitting of the peak profile and refined parameters from the synchrotron radiation data are significantly better than those from rotating anode data. No significant differences are found between single crystal results and those in this work. This work provides evidence that powder diffraction, especially with synchrotron radiation, could be used as one means of structural analysis even for such a weakly scattering organic material.

INTRODUCTION

X-ray powder diffraction has been widely applied to characterize materials^{1,2} for which to grow a big enough single crystal for structural analysis is impossible. Sometimes, it may be needed to investigate certain particular physical properties of a powder specimen which may not exist in the corresponding single crystal form. The aim of the Rietveld method is to produce structural parameters from powder diffraction data. It was originally proposed^{3,4} to avert some difficulties associated with peak overlapping in neutron diffraction of powder specimens. Recently, it has been applied extensively to X-ray diffraction with either a conventional source⁵ or with synchrotron sources.⁶⁻⁸ Of over 280 programs⁹ in existence for analysis of powder diffraction data, Rietveld method is considered to be one of the most popular ones. A joint project on the Rietveld refinement of $PbSO_4$ with both X-ray and neutron powder diffraction was initiated by the Commission on Powder Diffraction of IUCr (International Union of Crystallography); the results were compared in detail by Hill.¹⁰ In his report, it was clearly indicated that the refinement procedure was by no means trivial.

A combination of high-resolution powder diffraction and Rietveld method has been applied successfully on metal alloys and simple inorganic solid state compounds,^{1,7,8,10} mainly because of the strong scattering power and relatively simple structures of the materials. In other words, there are generally only a few parameters which can be varied because of constraints from the crystal symmetries. Recently, such a technique has been widely applied to zeolite structures¹¹ in which the frame-work is always known to be rigid; therefore the variables are restricted to only those "guest molecules". Only a few organic samples have been studied by such a method.^{6,12} Because of the relatively weak scattering power of an organic substance, a more intense X-ray source is needed to produce good enough powder diffraction data for structural refinement. Although some authors claimed that structural determination could be made even with low-resolution powder diffraction data,¹² synchrotron radiation as an X-ray source proved a much more promising source for such work.

The galvinoxyl radical (1) is one of the most important ferromagnetic organic substance.¹³⁻¹⁷ Single crystal of such a compound was reported to exhibit strong paramagnetism above 85 K,¹⁸ however the freeze-dried fuzzy fine powder



form of this compound exhibited different magnetic properties. Systematic studies on the suppressed freeze-dried samples showed an intrinsic paramagnetic to diamagnetic transition.¹⁹ Therefore, it is of interest to investigate the structure of such a powder form to compare with that of single crystal in order to understand their different behaviors in magnetic properties. This investigation provides a practical example on the feasibility of such a method applied to a complicated organic molecule. Powder diffraction patterns were obtained with both a rotating anode source and synchrotron radiation with similar wavelength in the hope to provide a useful comparison in terms of radiation sources.

EXPERIMENTAL SECTION

XRD Data Collection

Powder specimens of galvinoxyl radicals were prepared by a freeze-dry technique at 5 °C using a highly dilute benzene solution.¹⁹ Samples were first placed in a beryllium cell of dimensions approximately 10 × 20 × 1 mm. It was then mounted on a Huber 5020 diffractometer at X10B of the NSLS (National Synchrotron Light Source) at BNL (Brookhaven National Laboratory). A bent triangular Ge(111) crystal was used to produce monochromatic beam at wavelength 1.5855 Å, which was calibrated by a polycrystalline specimen of silicon SRM 640B.

The complete diffraction pattern was recorded in a vertical plane with $\theta/2\theta$ scan from 2θ 7.5° to 66.25° in steps 0.01° using fixed monitor counts.²⁰ The total duration of data collection was 16 h. This data set will be referred later in the text as SR data set. Cu K α X-ray powder diffraction data was recorded on a rotating anode (Rigaku 18 KW) with a similar procedure. A graphite monochromator coupling with precision slits (Huber 3013) and a diffractometer (Huber 422) were used to collect the powder pattern from 2θ 6° to 45° in steps 0.03°. The total duration of data collection was 72 h. This data set will be referred as RA data set.

RIETVELD METHOD

A physical description of the Rietveld method would be structural refinement based on whole pattern fitting. Instead of deriving the relative integrated intensity of a particular Bragg reflection after resolving the overlap problem, one starts with a reasonable model of the structure and some parameters of the pattern to derive an initial calculated powder pattern. The fitting procedure was then processed to minimize the differences between the observed and calculated patterns by means of least-squares refinement. The parameters to be refined include peak width, profile function, instrumental parameters, cell parameters, background, atomic coordinates, thermal parameters etc.

As in any other least-squares refinement, the quantity minimized is the weighted sum of the squares of the differences between observed and calculated intensities at each step.

$$wRp = \sum_i w_i |Y_{i\text{obs}} - Y_{i\text{cal}}| / \sum_i (Y_{i\text{obs}})$$

where, Y_i is the intensity at step i , Y_{obs} and Y_{cal} are observed and calculated values respectively; w_i is the weight associated with step i . Y_i may contain contributions from several Bragg reflections, such as

$$Y_{i\text{cal}} = s \sum_k M_k L_k |F_k|^2 P_k O_k + Y_{i\text{bgd}}$$

where, s is a scale factor, \sum_k means the sum over all k Bragg reflections; M is the multiplicity factor, L is the Lorentz and polarization factor, F is the structure factor, P is the reflection profile function, O is the preferred orientation function, $Y_{i\text{bgd}}$ is the background counts at step i .

REFINEMENT PROCEDURE

Rietveld refinement of powder data was performed with the GSAS²¹ program on a μ VAX computer. The initial model was taken from the single crystal structure.²² In the initial stage, atomic coordinates and thermal parameters were fixed at their starting values, and the scale factor, background, instrumental parameters, peak width and cell parameters were refined based on only the low angle part of the pattern (7° ~ 45°). After the convergence of all these parameters, refinement including atomic parameters and isotropic thermal parameters of non-H atoms was performed based on the full range of data points. For all H atoms, the

positional parameters were fixed at SC values and u_{iso} were also fixed at 0.05 during refinement. The agreement index Rp was 0.11 at this stage for SR data. The parameters of the profile function were then carefully added into the refinement until they were converged. The peak shape was approximated with a pseudo-Voigt profile function. As refinement proceeded, it was necessary to include a preferred orientation correction of the $\langle 011 \rangle$ direction for this needle-like crystal. For RA data, the atomic parameters were fixed at the values obtained from SR data during refinement. The final agreement indices were converged to $R_p = 0.08$, $wR_p = 0.11$ and $R_p = 0.17$, $wR_p = 0.21$ respectively for SR and RA data sets.

RESULTS AND DISCUSSION

The profiles of the (400) reflection from both SR and RA data sets are displayed in Fig. 1. It is obvious that the data quality and profile fitting of the SR data are much better

than those of the RA data. The full width at half maximum (FWHM) of the (400) reflections are 0.069° and 0.243° for SR and RA data respectively. The profile of this reflection is also more symmetric for the SR data than for the RA data. Counting statistics for intensity are a hundred times greater for SR data (10^4) than for RA data (10^2), even with a different time scale at each step; the time spent at each data point for SR data is 0.055 that for RA data. The powder pattern of SR and RA data up to $2\theta = 46^\circ$ are shown in Fig. 2 and 3 respectively. In order to clarify the large difference in relative intensities between the low and high angle parts in such an organic material, the patterns are displayed in two parts: the low angle part from 7.5° to 26° in 2θ for relative high intensities (10^4 for SR; 10^2 for RA); the high angle part from 26° to 46° for relative low intensities (10^2 for SR; 10^1 for RA). The fitting of SR data is significantly better than that of RA data especially in the high angle part. This fact is also indicated in the agreement indices with much smaller Rp and wRp values for SR data than those for RA data.

Of course with a smaller step size and with wider 2θ

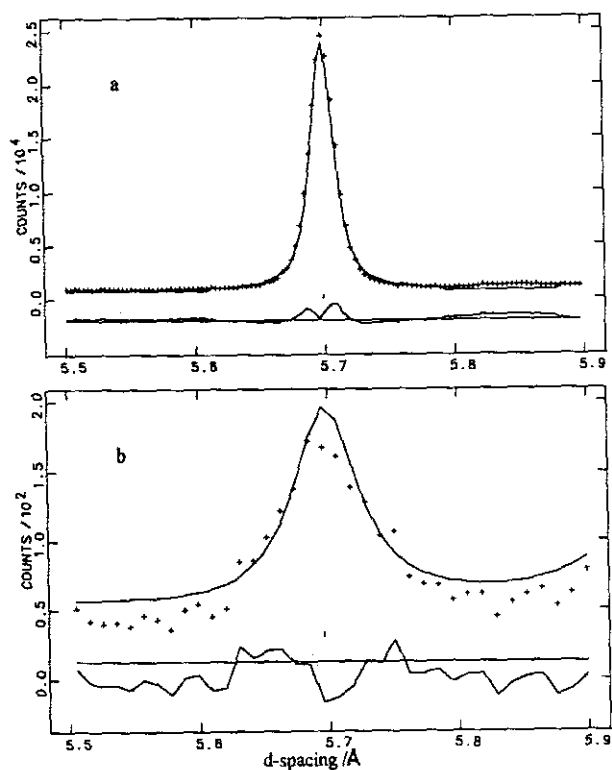


Fig. 1. Profile of (400) reflection with solid line from fitting of FWHM and (+) as measured data points. The horizontal axis is in d-spacing/Å in order to compare the two experiments; the vertical axis is in counts/step. The bottom curve shows the difference $Y_{obs} - Y_{cal}$. (a) SR data; FWHM = 0.069° (b) RA data with FWHM = 0.243° .

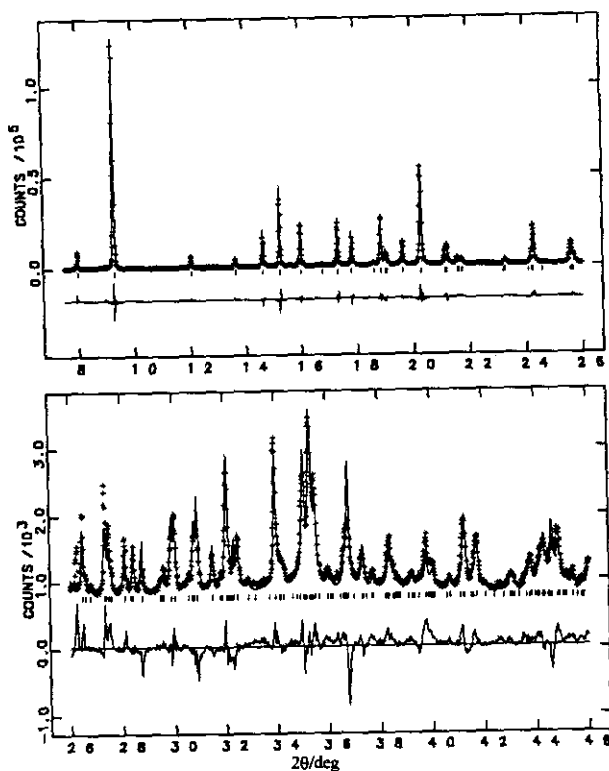


Fig. 2. Powder pattern of SR data, solid line and (+) signs are defined as for Fig. 1. Tick marks under the profile indicate the positions of Bragg reflections. The horizontal axis is in degrees of 2θ ; the vertical axis is in counts/step * 10^5 for the low angle part and * 10^3 for the high angle part.

range in SR data, there are far more data points in the SR data set than in the RA data set; this effect may contribute the better results. A comparison of some essential parameters and experimental conditions of the two data sets as well as the single crystal work are given in Table 1. The typical standard deviation in cell dimensions is one tenth for SR data that for RA data. An ORTEP plot based on the SR data refinement is shown in Fig. 4. Refinement of atomic parameters from RA data was unsuccessful.

Since the structural parameters obtained from the powder sample are the same as those in the single crystal form within the standard deviations shown in Tables 2 and 3. The anomalies in magnetic properties of the powder specimen with respect to the single crystal form cannot be easily correlated with the molecular structure. The magnetic behavior may well result from a more complicated interaction between particles, such as the cooperative effect of long-range spin interactions.

Although this is a refinement on a known structure of an organic material with 16 non-H atoms, it is conceivable that a careful powder diffraction measurement, especially with high-resolution by means of synchrotron radiation

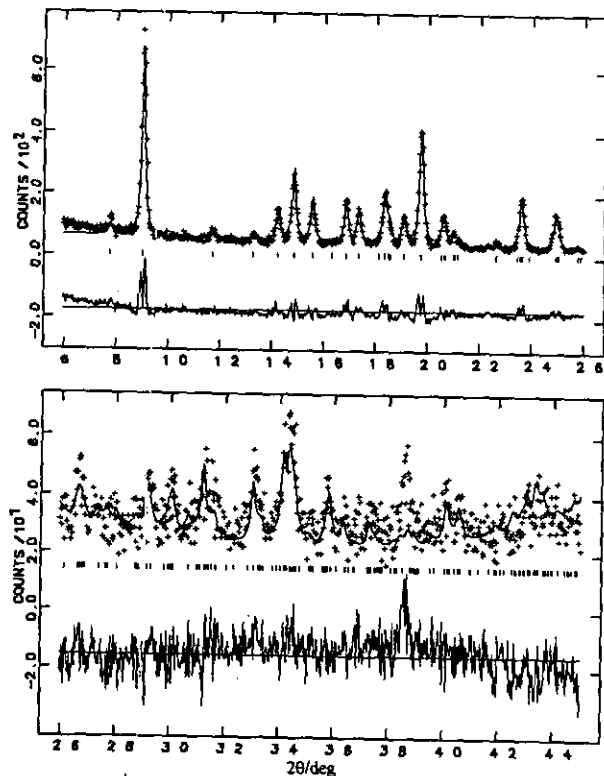


Fig. 3. Powder pattern of RA data; all definitions are as for Fig. 2. The vertical axis is in counts/step * 10^2 for the low angle part and * 10^1 for the high angle part.

Table 2. Comparison of Non-H Atomic Parameters for (a) SR Powder and (b) Single Crystal²² Data

Atom		x	y	z	U_{iso}
O	(a)	0.3315(6)	0.137(1)	-0.173(1)	0.098(5)
	(b)	0.3302(1)	0.1386(2)	-0.1739(2)	0.120(1)
C1	(a)	0.368(1)	0.096(4)	-0.080(2)	0.070(9)
	(b)	0.3688(1)	0.1005(3)	-0.0791(3)	0.067(1)
C2	(a)	0.373(1)	-0.032(4)	-0.044(2)	0.067(9)
	(b)	0.3728(1)	-0.0320(2)	-0.0446(2)	0.056(1)
C3	(a)	0.416(2)	0.066(2)	0.059(3)	0.056(8)
	(b)	0.4175(1)	-0.0687(2)	0.0586(2)	0.061(1)
C4	(a)	0.460(1)	0.013(1)	0.139(2)	0.072(9)
	(b)	0.4594(1)	0.0132(2)	0.1393(2)	0.057(1)
C5	(a)	0.451(1)	0.137(4)	0.103(3)	0.095(9)
	(b)	0.4559(1)	0.1403(2)	0.1028(2)	0.058(1)
C6	(a)	0.413(2)	0.187(2)	0.002(2)	0.10(1)
	(b)	0.4127(1)	0.1862(2)	0.0020(2)	0.058(1)
C7	(a)	1/2	-0.038(2)	1/4	0.12(1)
	(b)	1/2	-0.0384(3)	1/4	0.065(1)
C8	(a)	0.3261(9)	-0.120(2)	-0.122(2)	0.060(8)
	(b)	0.3261(1)	-0.1205(3)	-0.1230(1)	0.063(1)
C9	(a)	0.3332(8)	-0.254(2)	-0.075(2)	0.086(8)
	(b)	0.3380(2)	-0.2523(4)	-0.0744(4)	0.118(1)
C10	(a)	0.3228(9)	-0.121(2)	-0.267(2)	0.093(8)
	(b)	0.3226(2)	-0.1180(4)	-0.2683(3)	0.096(1)
C11	(a)	0.2699(8)	-0.082(2)	-0.109(2)	0.096(9)
	(b)	0.2661(1)	-0.0834(4)	-0.1089(4)	0.108(1)
C12	(a)	0.406(1)	0.325(2)	-0.030(2)	0.066(8)
	(b)	0.4068(1)	0.3239(3)	-0.0291(3)	0.070(1)
C13	(a)	0.4558(8)	0.395(2)	0.070(2)	0.118(9)
	(b)	0.4532(2)	0.3988(3)	0.0706(4)	0.094(1)
C14	(a)	0.3473(8)	0.371(2)	0.022(2)	0.094(9)
	(b)	0.3467(2)	0.3706(3)	-0.0228(4)	0.101(1)
C15	(a)	0.4144(8)	0.347(2)	-0.162(2)	0.094(9)
	(b)	0.4140(2)	0.3498(4)	-0.1653(3)	0.108(1)

measurements, might provide structural information for normal organic substances. The result of this work is cer-

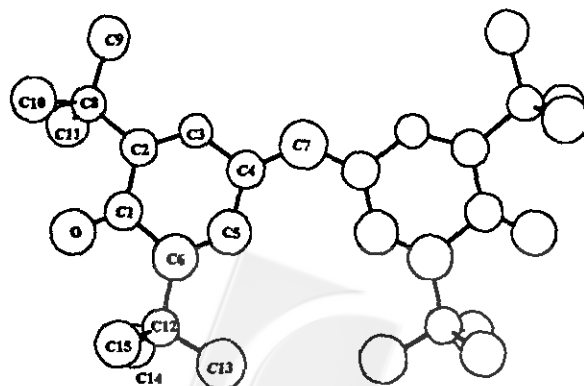


Fig. 4. Molecular structure drawing with parameters refined on SR data.

Table 1. Crystal Data and Experimental Conditions of SR, RA and Single Crystal Data Sets

	SR	RA	SC ²²
Formular	C ₂₉ H ₄₁ O ₂	C ₂₉ H ₄₁ O ₂	C ₂₉ H ₄₁ O ₂
Space group	C 2/c	C 2/c	C 2/c
Z	4	4	4
a/Å	23.786(1)	23.76(1)	23.733(4)
b/Å	10.8611(4)	10.856(6)	10.843(2)
c/Å	10.6766(4)	10.666(4)	10.666(2)
β/deg	106.634(3)	106.62(2)	106.64(2)
Wavelength/Å	1.5855	1.5418 (Cu Kα)	1.5418 (Cu Kα)
2θ ranges/deg	7.5 ~ 66.25	6 ~ 45	3. ~ 120.
Step size in 2θ/deg	0.01	0.03	-
time/step/s	~10	~180	-
# of data points	5696	1333	-
# of integrated reflections	490	189	1959
# of variables	82	20	162
Total data time/h	16	72	14
# of profile parameters	9	9	-
O, <011>	1.02	1.02	-
R _p	0.08	0.17	0.051
wR _p	0.11	0.21	0.069
Typical std. dev. of positional parameters	0.002	-	0.0002
Typical std. dev. of thermal parameters, (U _{iso})	0.009	-	0.001

SC: single crystal data

O: preferred orientation

R_p = (Σ_i|Y_{i,obs} - Y_{i,calc})/Σ_iY_{i,calc}wR_p = (Σ_iw_i|Y_{i,obs} - Y_{i,calc})/Σ_iY_{i,calc}Y_i: intensity at *i*th step, w: weightTable 3. Selected Bond Lengths/Å and Bond Angles/deg for (a) SR Powder and (b) Single Crystal²² Data

O-C1	(a) 1.20(3)	C4-C5	(a) 1.40(3)
	(b) 1.226(3)		(b) 1.429(4)
C1-C2	(a) 1.43(2)	C4-C7	(a) 1.41(2)
	(b) 1.479(4)		(b) 1.408(3)
C1-C6	(a) 1.53(3)	C5-C6	(a) 1.32(3)
	(b) 1.476(3)		(b) 1.351(3)
C2-C3	(a) 1.351(3)	C2-C8	(a) 1.53(3)
	(b) 1.32(2)		(b) 1.522(3)
C3-C4	(a) 1.43(2)	C6-C12	(a) 1.53(3)
	(b) 1.424(3)		(b) 1.527(4)
∠O-C1-C2	(a) 125(2)	∠O-C1-C6	(a) 117(2)
	(b) 120.7(2)		(b) 120.5(3)
∠C1-C2-C3	(a) 119(2)	∠C2-C1-C6	(a) 118(3)
	(b) 117.9(2)		(b) 118.8(2)
∠C1-C2-C8	(a) 117(3)	∠C3-C2-C8	(a) 123(3)
	(b) 119.4(2)		(b) 122.7(2)
∠C2-C3-C4	(a) 126(2)	∠C3-C4-C5	(a) 115(3)
	(b) 123.9(2)		(b) 117.4(2)
∠C3-C4-C7	(a) 118(2)	∠C5-C4-C7	(a) 128(3)
	(b) 116.8(2)		(b) 125.7(2)
∠C4-C5-C6	(a) 129(3)	∠C1-C6-C12	(a) 119(3)
	(b) 123.0(2)		(b) 118.9(2)
∠C4-C7-C4'	(a) 134(2)	∠C5-C6-C12	(a) 126(3)
	(b) 133.2(3)		(b) 122.3(2)

tainly encouraging in that it is possible to do the structural determination of an organic molecule based on powder diffraction data in the near future.

CONCLUSION

The combination of synchrotron radiation powder diffraction measurement and the Rietveld method provides a powerful tool to obtain structural information of an organic substance. The improvement of data quality from rotating anode source to synchrotron radiation source at roughly the same wavelength is great. Its importance for structural refinement is clearly demonstrated.

ACKNOWLEDGMENT

We thank Dr. K. S. Liang of EXXON Corporate Research for access to the synchrotron and rotating anode experiments as well as for helpful discussions.

Received August 26, 1994.

Key Words

Synchrotron Radiation; Rietveld method; Galvinoxyl.

REFERENCES

1. Cox, D. E.; Hastings, J. B.; Thomlinson, W.; Prewitt, C. T. *Nucl. Instrum. Methods*, **1983**, 208, 573.
2. Cheetham, A. K.; Wilkinson, A. P. *Angew. Chem. Int. Ed. Engl.* **1992**, 31, 1557.
3. Rietveld, H. M. *Acta Cryst.* **1967**, 22, 151.
4. Rietveld, H. M. *J. Appl. Cryst.* **1969**, 2, 65.
5. Deboer, B. G.; Young, R. A.; Sakhivel, A. *Acta Cryst.* **1994**, C50, 476.
6. Cernik, R. J.; Cheetham, A. K.; Prout, C. K.; Watkin, D. J.; Wilkinson, A. P.; Willis, T. M. *J. Appl. Cryst.* **1991**, 24, 222.
7. Morris, R. E.; Harrison, T. A.; Nicol, J. M.; Wilkinson, A. P.; Cheetham, A. K. *Nature*, **1992**, 359, 519.
8. La Placa, S. J.; Bringley, J. F.; Scott, B. A.; Cox, D. E. *Acta Cryst.* **1993**, C49, 1415.
9. Smith, D. K.; Gorter, S. *J. Appl. Cryst.* **1991**, 24, 369.
10. Hill, R. J. *J. Appl. Cryst.* **1992**, 25, 589.
11. Lin, J. C.; Chao, K. J.; Wang, Y. *Zeolites*, **1991**, 376.
12. Wilson, C. C.; Wadsworth, J. W. *Acta Cryst.* **1990**, A46, 258.
13. Iwamura, H. *Advances in Physical Organic Chemistry*; Academic: New York, **1990**.
14. Bock, H.; John, A.; Havlas, Z.; Bats, J. W. *Angew. Chem. Int. Ed. Engl.* **1993**, 32, 416.
15. Morton, J. R.; Preston, K. F.; Le Page, Y.; Williams, A. J.; Word, M. D. *J. Chem. Phys.* **1990**, 93, 2222.
16. Williams, D. E. *Mol. Phys.* **1969**, 16, 145.
17. Chi, K. M.; Calabrese, J. C.; Miller, J. S.; Khan, S. I. *Mol. Cryst. Liquid Cryst.*, **1989**, 176, 185.
18. Mukai, K. *Bull. Chem. Soc., Jpn.* **1969**, 42, 40.
19. Chiang, L. Y.; Upasani, R. B.; Sheu, H. S.; Goshorn, D. P.; Lee, C. H. *J. Chem. Soc., Chem. Commun.* **1992**, 959.
20. Because the ring current of synchrotron radiation is normally decayed in time, the monitor mode is applied so that the number of incident photons is kept the same at each step.
21. Larson, A. C.; Von Dreele, R. B. GSAS, *Generalized Crystal Structure Analysis System* **1987**, Report. LAUR-86-748, Los Alamos National Laboratory, Los Alamos, NM, U. S. A.
22. Crystalalytics Company, reference code: CDB1-0290. Lincoln, Nebraska, **1990**.

